Plasma Phys. Control. Fusion **50** (2008) 055005 (8pp) doi:10.1088/0741-3335/50/5/055005

Sheared flow generation and mode suppression in a magnetized linear cylindrical plasma

H Tsuchiya[1], S-I Itoh[2], A Fujisawa[3], K Kamataki[4], S Shinohara[4], M Yagi[2], Y Kawai[2], A Komori[3] and K Itoh[3]

[1] School of Physical Sciences, Graduate University for Advanced Studies, Toki 509-5292, Japan
[2] Research Institute for Applied Mechanics, Kyshu University, Fukuoka 816-8580, Japan
[3] National Institute for Fusion Science, Toki 509-5292, Japan
[4] Interdisciplinary Graduate School of Engineering Sciences, Kyushu University, Fukuoka 816-8580 Japan

E-mail: tsuchiya.hayato@lhd.nifs.ac.jp

Received 5 November 2007, in final form 13 February 2008
Published 10 March 2008
Online at stacks.iop.org/PPCF/50/055005

Abstract

In a magnetized cylindrical plasma produced with the electron cyclotron resonance (ECR) scheme, a sheared $E \times B$-flow showing zonal flow (ZF) characteristics has been driven by ECR power modulation. This method was used to control the sheared flow, and allowed us to observe that a coherent mode (spontaneously driven in the plasma) becomes stabilized as the induced plasma flow amplitude increases. The stabilization of the mode is caused by the increase in the plasma flow shear; thus, the result demonstrates the fundamental process of the shearing effect of ZFs on turbulence, which is commonly observed in toroidal plasma confinement devices for fusion research.

(Some figures in this article are in colour only in the electronic version)

1. Introduction

Nonlinear interaction between drift waves (DWs) and zonal flows (ZFs) has attracted attention in plasma physics [1–3]. The ZFs are constant on magnetic surfaces but change flow directions radially. According to theories and nonlinear simulations, the ZFs modulate microscopic fluctuations (such as DWs, interchange mode and ion temperature-gradient driven mode), and suppress turbulence-driven transport in magnetically confined plasmas. Therefore, quantitative prediction of the turbulent transport in confined plasmas requires improved knowledge of the system of microscopic fluctuations and meso-scale ZFs.

To date, the presence of ZFs has been confirmed in toroidal plasmas and linear plasmas, and experiments on nonlinear interaction between DWs and ZFs have been reported recently [4–15]. (See, for a review of experiment [16].) These observations, however, have been given for limited values of ZF intensity, since the ZFs are generated by the background turbulence

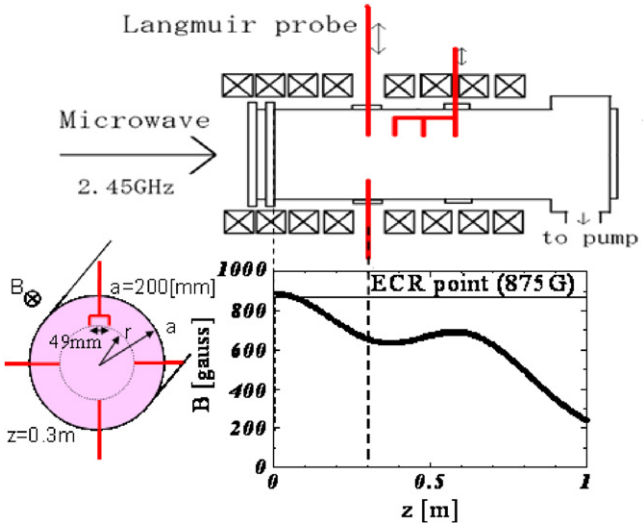

Figure 1. A schematic diagram of the experimental set-up, probe configuration and magnetic field configuration.

itself. Therefore, quantitative understanding of the nonlinear interaction between DWs and ZFs requires experiments in which ZFs are driven in a controlled manner. Pioneering works on the influence of sheared flow on turbulence were reported in [17–19] where the mean radial electric field was controlled by the biased limiter. The impacts on turbulence were studied, and have stimulated further detailed studies on the nonlinear interaction of fluctuations.

Recently a novel experimental method has been developed to drive a ZF in a linear mirror device in Kyushu University. The plasma is produced by the electron cyclotron resonance (ECR) scheme and is confined in a linear mirror field. In the plasma, a coherent mode presumed as flute instabilities inherently exists in the region of unfavorable magnetic curvature [20]. By applying the ECR power modulation, we successfully generate the circularly symmetric perturbation of the electrostatic potential. The generated flow pattern shows the ZF characteristics, which means being constant along the magnetic field and changing its sign in the radial direction. Using the novel method, we have successfully observed that the native instability mode is distorted by the induced ZFs, and the fluctuation level is reduced as a consequence of the induced ZFs. In this paper we present a method to generate the ZFs (i.e. sheared flow structure), the modulation of the spontaneous instability, stretching of the mode pattern and the suppression of fluctuations, i.e. fundamental processes of the $E \times B$-shearing effect of ZFs on fluctuations.

2. Experimental methods

The experiments were performed in a cylindrical mirror device [20]. As is shown in figure 1, the diameter and the length of the produced plasma are 40 cm and 120 cm, respectively. In this device, the plasma is produced with ECR scheme using a magnetron. The frequency and the maximum power of the magnetron are 2.45 GHz and 1 kW, respectively. ECR power can be modulated with an external control signal with a frequency of up to 13 kHz. The corresponding resonance magnetic field strength is 875 G at $z = 5.5$ cm, where the origin of z is the left edge of the chamber in figure 1.

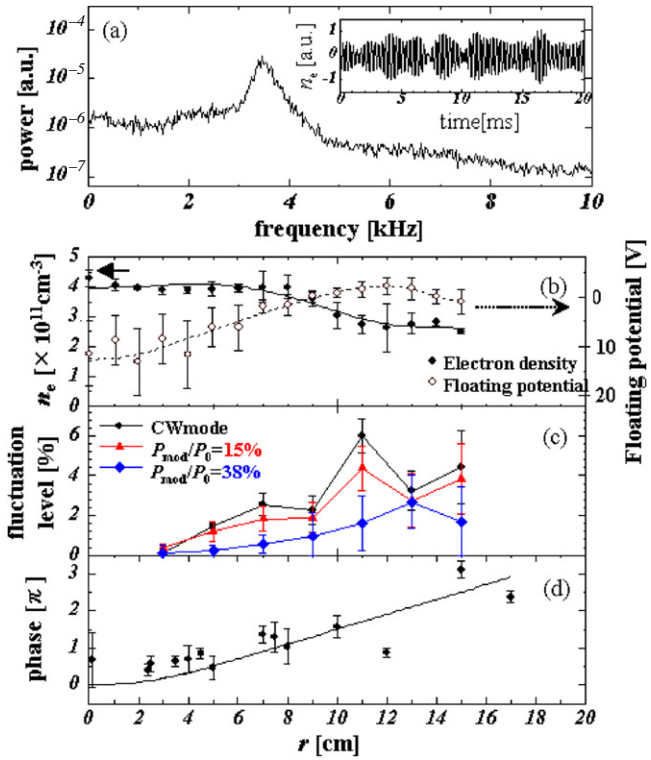

Figure 2. Characteristics of the native mode. (*a*) Power spectrum of density fluctuation and the inset showing a typical waveform of the native mode with a band-pass filter in the frequency range 3–4.5 kHz. (*b*) Radial density profile (solid line, left axis) and floating potential (dashed line, right axis) of the background plasma. (*c*) The fluctuation level of the native mode, which is evaluated by the integrated fluctuation amplitude in the frequency range 3–4.5 kHz. (*d*) Radial phase shift of the native mode referred to the radial position at $r \sim 0.15$ cm.

Argon is chosen as the plasma species for this experiment. The target plasma is produced with an ECR power of 400 W, and the resultant density and electron temperature are $n_e \sim 10^{11}$ cm^{-3} and $T_e \sim 4$ eV, respectively. These plasma parameters are measured with Langmuir probes. The probe characteristic has no sign of non-thermal contribution in this plasma condition.

All the poloidal probes can be moved in the radial direction to measure the radial profiles of the plasma parameters. Five probes are installed to measure different azimuthal positions ($\theta = 0°$, 90°, 180°, 256° and 284°) on the same radius at $r = 10$ cm (figure 1). Four probes are set at different positions along the longitudinal direction. These probe signals are digitized with a frequency of 100 kHz, and thus, the corresponding Nyquist frequency is 50 kHz. In the present experiments, we assume that the ion saturation current is proportional to the plasma density.

3. Results

3.1. Observation of the spontaneous fluctuation

A specific feature of the plasma is that a coherent mode, called native mode in this paper, is spontaneously excited at a frequency of 3.7 kHz . Figure 2(*a*) shows a power spectrum of ion

saturation current at $r = 11$ cm. A sharp peak at 3.7 kHz is obvious in the spectrum. The inset in figure 2(*a*) demonstrates the temporal behavior of the mode extracted using the band-pass filter from the signal of ion saturation current. As seen in the inset of figure 2(*a*), the native mode shows an intermittent nature with a typical lifetime of several milliseconds.

The azimuthal array of the Langmuir probes indicates that the poloidal mode number of the native mode is $m = 2$, and that it propagates in the ion diamagnetic direction. The axial array shows that the native mode is uniform along the magnetic field. Using a movable probe, the radial profile of the density and floating potential (figure 2(*b*)) and its denstity fluctuation (figure 2(*c*)) accompanied with the mode can be evaluated on a shot-by-shot basis. The radially movable probe measurement shows the radial propagation of the mode. The phase delay to a reference probe signal, which is located at $r = 0.15$ cm, indicates that the radial wavelength should be approximately 12 cm (see figure 2(*d*)). The radial profile of the mode, shown in figure 2(*c*), demonstrates that the fluctuation amplitude has a maximum around $r = 11$ cm, where the steep density gradient exists (see figure 2(*b*)). It has also been confirmed that the phase between the density fluctuation and the potential fluctuation is out of phase at the same point. The observed features are consistent with those of the flute instability [20].

The measurement of the Langmuir probes indicates that the radial profile of the plasma space potential takes a negative parabolic form. This background flow gives a significant Doppler effect in the observation of the native mode in the laboratory frame. The plasma rotates in the electron diamagnetic direction with an angular velocity of 4.1 kHz and hence the real frequency of the native mode in the plasma frame is deduced to be 11.9 kHz by taking into account the $m = 2$ property of the mode. Nevertheless the background $E \times B$ flow does not give any significant distortion or shearing effect to the native mode, because the plasma rotation is considered almost as a rigid body rotation.

3.2. Excitation of artificial zonal flows

A power modulation expressed as $P_{\mathrm{ECR}} = P_0 + P_{\mathrm{mod}} \sin(2\pi f_{\mathrm{mod}} t)$ can be applied on this plasma. Here, P_0 and P_{mod} represent the DC and modulation powers, respectively. The maximum modulation is approximately 50%, where the modulation level is defined as P_{mod}/P_0. It is found that the plasma parameters change in a synchronized manner with the power modulation. In particular, the plasma potential or the radial electric field is clearly modulated with a good reproducibility. In other words, the background plasma poloidal flow can be modulated in a time-dependent manner by controlling the ECR power. In this paper, the modulated pattern of the plasma structure is termed *modulator*.

The modulator intensity increases with the power modulation level P_{mod}/P_0 in the available range of modulation frequency from 1 to 13 kHz. A good reproducibility allows us to evaluate a typical temporal evolution of the structure by making the conditional average using the external power modulation signal as a clock. The probe measurements reveal that the structural change with the modulator shows a symmetric nature around the plasma center, and it propagates radially outwards synchronized with the modulation. The modulator is also found to contain higher harmonic frequencies. The fraction of the 3rd harmonics to the fundamental one is less than 6% at the maximum ($r = 9$ cm, $f_{\mathrm{mod}} = 1$ kHz, $P_{\mathrm{mod}}/P_0 = 38\%$), while the fourth harmonics amplitude is buried in the background level.

Figure 3 shows an example of the typical evolution of the modulator in the case of $f_{\mathrm{mod}} = 1$ kHz. The lines in figure 3 represent the instant modulator field, obtained as the conditional average, at $t = 0$, $T_{\mathrm{mod}}/4$, $T_{\mathrm{mod}}/2$ and $3T_{\mathrm{mod}}/4$, where T_{mod} denotes the period of the modulation. As shown in figure 3, the amplitudes of the potential perturbation and electric

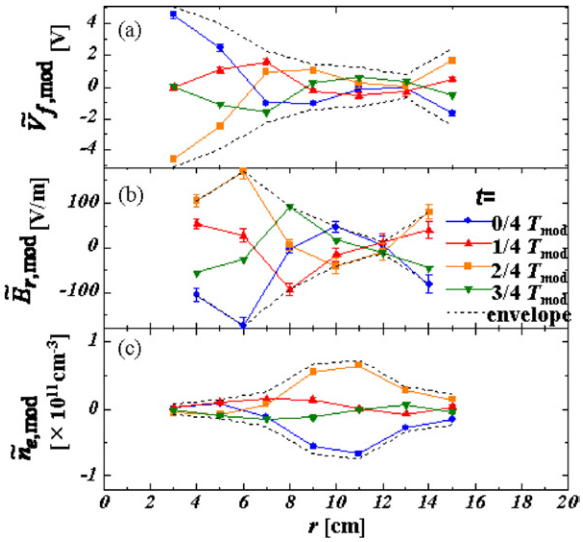

Figure 3. Typical time evolutions of modulator field at $f_{\mathrm{mod}} = 1\,\mathrm{kHz}$, $P_0 = 400\,\mathrm{W}$ and $P_{\mathrm{mod}}/P_0 = 38\%$. (*a*) Radial profiles of fluctuating parts of floating potential, (*b*) electric field and (*c*) density at four times at $t = 0$, $T_{\mathrm{mod}}/4$, $T_{\mathrm{mod}}/2$ and $3T_{\mathrm{mod}}/4$.

field (accompanied with the modulator) become large towards the axis, while the density fluctuation level has the maximal value around 10 cm.

3.3. Wave coupling and reduction

It is possible using the method to investigate how the native mode is changed by increasing the ZF intensity induced by the modulator. Figure 4 shows the change in the native mode in the power spectrum at $r = 9\,\mathrm{cm}$ for four different cases in the modulation power when 1 kHz modulator is induced. From the figures, it is clear that the native peak becomes broader and side band peaks appear as the modulation level increases. The poloidal modes of the side band peak around 2.7 kHz are confirmed to be $m = 2$, and therefore, the side band peaks satisfy the coupling condition, i.e. $f_{\mathrm{sum,sub}} = f_{\mathrm{coh}} \pm f_{\mathrm{mod}}$ and $k_{\mathrm{sum}} = k_{\mathrm{coh}} + k_{\mathrm{mod}}$. This result clearly demonstrates that the modulator should suppress the native mode through the nonlinear excitation of the stable quasimodes at f_{sub} and f_{sum}.

Figure 4(*e*) shows the dependence of the native mode amplitude on the induced ZF amplitude normalized by $\omega_{\mathrm{mod}}/k_{\theta,\mathrm{mod}}$. The explicit form of the normalized parameter is defined here as $\alpha = k_{\theta,\mathrm{mod}} v_{E\times B}/\omega_{\mathrm{mod}} = mE_r/r\omega_{\mathrm{mod}}B$. As clearly shown in this figure, the native mode amplitude is reduced with an increase in the induced flow, particularly, the reduction becomes clear when the normalized parameter goes above one. This result can be interpreted as that the effect of the suppression becomes significant when the running distance of the induced poloidal flow during a period of the modulation becomes comparable to the wavelength of the native mode [21].

3.4. Shear flow distortion on spontaneous fluctuation pattern

Since both explicit temporal expressions of the modulator and the native mode are available, the distortion of the native mode pattern due to the background flow modulation can be

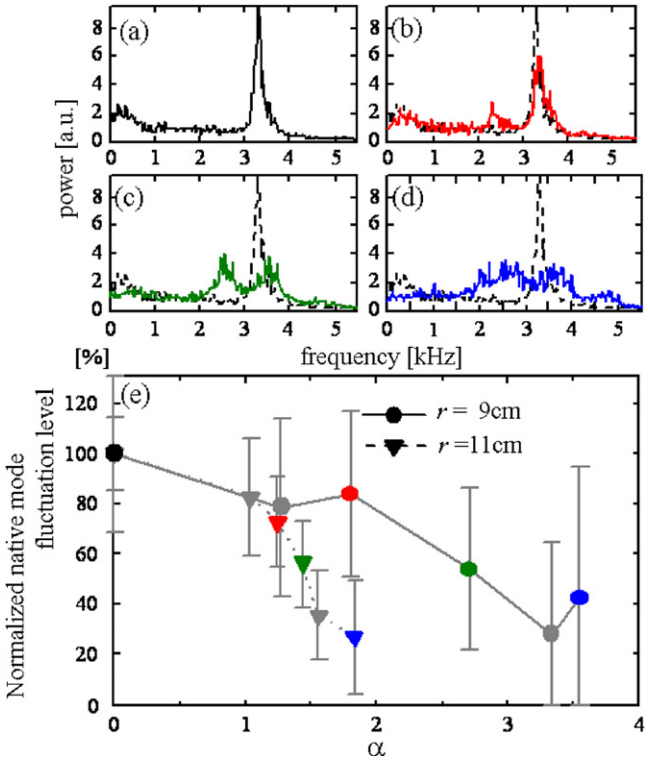

Figure 4. Change of native mode power in response to the increase in modulator intensity. The power spectra (*a*) without power modulation, (*b*) with the modulation of $P_{\mathrm{mod}}/P_0 = 15\%$, (*c*) $P_{\mathrm{mod}}/P_0 = 22\%$ and (*d*) $P_{\mathrm{mod}}/P_0 = 38\%$. The dashed line indicates the power spectrum without power modulation for reference. (*e*) Dependence of the native mode fluctuation level, normalized by the fluctuation level at $\alpha = 0$, on shearing rate or distortion of velocity field at $r = 9$ and 11 cm. The parameter α is an indicator of the intensity of the modulator electric field E_{r}. The color of the symbols corresponds to the case of the same modulation power shown in the above graphs. The gray symbols correspond to the other cases of modulation power.

inferred. The native mode of density fluctuation without modulator should be $\tilde{n}_{\mathrm{nm}}(r,t) = \tilde{n}^{\mathrm{E}}_{\mathrm{nm}}(r)\sin(k_r r + m\theta - \omega_{\mathrm{coh}}t)$, with the envelope function evaluated with the experimental data using the linear interpolation. In the case of the power modulation applied, the influence of advection by modulator is illustrated. If the original mode structure is assumed to be frozen to the flowing plasma, the distorted native mode pattern in the laboratory frame is described as $\tilde{n}_{\mathrm{nm}}(r,t) = \tilde{n}^{\mathrm{E}}_{\mathrm{nm}}\sin(k_r r + m\theta - \omega_{\mathrm{coh}}t - \Pi_{\mathrm{flow}}(r,t))$, where $\Pi_{\mathrm{flow}}(r,t) = m\int(v_{E\times B}/r)\,\mathrm{d}t$ is evaluated using the expansion of the harmonics of the fundamental modulator frequecy, as $v_{E\times B} = \sum_j v^{\mathrm{mod}}_{E\times B,j}(r)\sin(\delta^{\mathrm{mod}}_j(r) - j\omega_{\mathrm{mod}}t)$, where $v^{\mathrm{mod}}_{E\times B,j}(r)$ and $\delta^{\mathrm{mod}}_j(r)$ are the envelope and phase of the jth harmonic components of the modulator, respectively.

Based on the experimental results, figure 5 illustrates reconstructed pattern (with froze-in assumption) corresponding to different modulation powers to give image plots of the interaction process between the native mode and the modulator. Here, the expression can include the lower-order components until the third harmonic. The images express snapshots of the patterns based on the above-mentioned mathematical expressions. The images clearly demonstrate that the original pattern of the mode suffers larger distortion, and that the radial wave number increases, as the induced flow intensity, or α, grows with the increase in the modulation power.

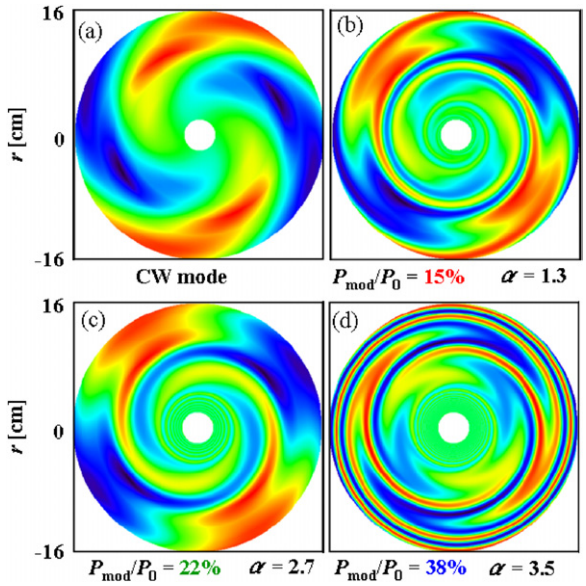

Figure 5. Image plots of the native mode distortion in the cases of (*a*) absence of modulator, (*b*) $P_{\mathrm{mod}}/P_0 = 15\%$, (*c*) $P_{\mathrm{mod}}/P_0 = 22\%$ and (*d*) $P_{\mathrm{mod}}/P_0 = 38\%$. The parameter α is an indicator of the degree of mode stretching.

4. Summary and discussions

It is worth discussing the effect of density profile change on the reduction of the native mode. As shown in figure 2(*b*), the density profile or density gradient is observed to change accompanied with the power modulation. The change in the linear growth rate can in principle affect the saturation level of the coherent mode. However, the maximum change in the density gradient is about 20%. This amount of the gradient change should not be sufficiently large to explain our observation, because the expected change in the linear growth remains to be approximately 10%, assuming that the growth rate is proportional to the square root of the gradient. Therefore, we conclude that the observed reduction of the native mode should be ascribed to the nonlinear interaction between the native mode and induced background ZFs, or the $E \times B$-shearing of background ZFs.

In summary, a novel method, to induce the ZF field in a controlled manner, has been developed in the ECR-produced cylindrical plasma. The background sheared flow was found to affect the inherently existing coherent mode in the plasma through the distortion of the mode pattern. The effect is equivalent to the $E \times B$-shearing mechanisms commonly observed in toroidal plasma confinement devices. Consequently, the observation presented in the paper is an instance to visualize the fundamental process of the $E \times B$-shearing mechanism.

Acknowledgments

The authors express their sincere thanks to Professor A Fukuyama and Professor P H Diamond for useful discussions and to Professor O Motojima for continuous encouragement. This work is partly supported by the Grants-in-Aid for Specially Promoted Research (16002005), by the collaboration programmes of RIAM Kyushu University and of NIFS (NIFS07KOAP017).

References

[1] Diamond P H, Itoh S-I, Itoh K and Hahm T S 2005 *Plasma Phys. Control. Fusion* **47** R35
[2] Rosenluth M N and Hinton F L 1998 *Phys. Rev. Lett.* **80** 724
[3] Lin Z, Hahm T S, Lee W W, Tang W M and Diamond P H 1999 *Phys. Rev. Lett.* **83** 3645
[4] Fujisawa A *et al* 2004 *Phys. Rev. Lett.* **93** 165002
[5] Xu G S *et al* 2003 *Phys. Rev. Lett.* **93** 125001
[6] Nagashima Y *et al* 2005 *Phys. Rev. Lett.* **95** 095002
[7] Tynan G R *et al* 2006 *Plasma Phys. Control. Fusion* **48** S51
[8] Sokolov V, Wei X, Sen A K and Avinash K 2006 *Plasma Phys. Control. Fusion* **48** S111
[9] Fujisawa A *et al* 2007 *J. Phys. Soc. Japan* **76** 033501
[10] Itoh K *et al* 1997 *Phys. Plasmas* **14** 020702
[11] Shats M G *et al* 2006 *Plasma Phys. Control. Fusion* **48** S17
[12] Mckee G *et al* 2003 *Phys. Plasmas* **10** 1712
[13] Conway G *et al* 2005 *Plasma Phys. Control. Fusion* **47** 1165
[14] Kramer-Flecken A *et al* 2006 *Phys. Rev. Lett.* **97** 045006
[15] Melnikov A V *et al* 2006 *Plasma Phys. Control. Fusion* **48** S87
[16] Fujisawa A *et al* 2007 *Nucl. Fusion* **47** S718
[17] Taylor R J *et al* 1989 *Phys. Rev. Lett.* **63** 2365
[18] Weynants R R *et al* 1998 *Plasma Phys. Control. Fusion* **40** 635
[19] Boedo J *et al* 2000 *Nucl. Fusion* **40** 1397
[20] Koga M, Tsuchiya H and Kawai Y 2005 *J. Phys. Soc. Japan* **74** 941
[21] Itoh K and Itoh S-I 1996 *Plasma Phys. Control. Fusion* **38** 1